Human-specific *ARHGAP11B* increases size and folding of primate neocortex in the fetal marmoset

Michael Heide[1]*, Christiane Haffner[1], Ayako Murayama[2,3], Yoko Kurotaki[4], Haruka Shinohara[4], Hideyuki Okano[2,3], Erika Sasaki[4], Wieland B. Huttner[1]*

[1]Max Planck Institute of Molecular Cell Biology and Genetics, 01307 Dresden, Germany. [2]Department of Physiology, Keio University School of Medicine, Tokyo 160-8582, Japan. [3]Laboratory for Marmoset Neural Architecture, RIKEN Center for Brain Science, Wako City, Saitama 351-0198, Japan. [4]Department of Marmoset Biology and Medicine, Central Institute for Experimental Animals, Kawasaki 210-0821, Japan.

*Corresponding author. Email: heide@mpi-cbg.de (M.H.); huttner@mpi-cbg.de (W.B.H.)

The neocortex has expanded during mammalian evolution. Overexpression studies in developing mouse and ferret neocortex have implicated the human-specific gene *ARHGAP11B* in neocortical expansion, but the relevance for primate evolution has been unclear. Here, we provide functional evidence that *ARHGAP11B* causes expansion of the primate neocortex. *ARHGAP11B* expressed in fetal neocortex of the common marmoset under control of the gene's own, human, promoter increased numbers of basal radial glia progenitors in the marmoset outer subventricular zone, increased numbers of upper-layer neurons, enlarged the neocortex, and induced its folding. Thus, the human-specific ARHGAP11B drives changes in development in the non-human primate marmoset that reflect the changes in evolution that characterize human neocortical development.

Evolutionary expansion of the human neocortex is linked to our cognitive abilities (*1–6*). The human-specific gene *ARHGAP11B* (*7, 8*) is implicated in this neocortical expansion as it is expressed in the human progenitor cells giving rise to neocortical neurons and, when overexpressed in developing mouse and ferret neocortex, two evolutionarily distant mammals, can induce features associated with neocortical expansion (*9, 10*). *ARHGAP11B* arose ≈5 mya by partial duplication of ubiquitous *ARHGAP11A*, which encodes a Rho-GAP exhibiting nuclear localization (*7–9, 11*). However, due to a point mutation that presumably occurred after the partial gene duplication event and leads to a human-specific change in protein sequence, ARHGAP11B lacks Rho-GAP activity in vivo and is localized in mitochondria, promoting proliferation of basal progenitors, the progenitors implicated in neocortical expansion, via glutaminolysis (*11, 12*). Here we tested ARHGAP11B's relevance for neocortical expansion in a non-human primate by expressing *ARHGAP11B* under the control of its own human promoter in transgenic fetal marmosets.

To express human-specific *ARHGAP11B* (*7, 8*) (fig. S1A) in the common marmoset, we constructed a lentiviral vector. In this functionally verified vector (fig. S1, B and C), a ≈2.7 kb human genomic segment containing the *ARHGAP11B* promoter drives expression of an EGFP reporter followed by the complete ARHGAP11B protein coding sequence. The two proteins become separate polypeptides after translation due to the presence of a T2A self-cleaving sequence (fig. S1B). This expression vector was used to generate pregnant marmosets carrying *ARHGAP11B*-transgenic fetuses, by following a previously established protocol (*13*) that involved microinjection into fertilized marmoset oocytes and transfer of in vitro developed embryos into foster mothers 3-5 days after ovulation (day of transfer being defined as day 0 of pregnancy; fig. S1D and table S1).

We confined our analyses to marmoset fetuses, because we anticipated that expression of this human-specific gene would affect neocortex development in the marmoset. In light of potential unforeseeable consequences with regard to postnatal brain function, we considered it a prerequisite – and mandatory from an ethical point of view – to first determine the effects of *ARHGAP11B* expression on the development of fetal marmoset neocortex. To this end, we collected fetuses after Caesarian section at day 101 of the ≈150-day gestation (fig. S1D), a stage when neocortical development shows both progenitor cell division and production of neurons (destined mostly to the upper layers) and which corresponds to fetal human neocortical development at ≈16 weeks post conception. Of the seven *EGFP*- plus *ARHGAP11B*-transgenic marmoset fetuses obtained (table S1), five expressed both EGFP and ARHGAP11B in fetal neocortex whereas two expressed neither (Fig. 1). In the five transgenic fetuses exhibiting EGFP and ARHGAP11B expression in neocortex, we found 3-4 lentivirus integration events at random genomic positions per animal (table S2). *ARHGAP11B* mRNA expression in the marmoset neocortical wall resembled that in fetal human neocortex, with similar intensity and occurring preferentially in the germinal zones (ventricular zone (VZ), inner subventricular zone (iSVZ), outer subventricular zone (oSVZ) (*14*)) (*9, 15*), like EGFP, as revealed by in-situ-hybridization (fig. S1E) and RT-qPCR (fig. S1F).

The *ARHGAP11B*-expressing marmoset neocortex was larger and its cortical plate (CP) thicker than normal marmoset neocortex (Figs. 1B and 2A and fig. S1E) and, in contrast to the smooth surface of the normal marmoset brain, exhibited surface folds (Fig. 2A). Quantification of fetal marmoset neocortex as a whole indicated no statistically significant difference in width but a significant increase in length of *ARHGAP11B*-expressing neocortex as compared to wild-type and *ARHGAP11B*-non-expressing neocortex (Fig. 2B). To quantify cortical folding, we analyzed coronal sections of fetal marmoset neocortex along the rostro-caudal axis (Fig. 2C) for the gyrification index (GI) (fig. S2A), the ratio of tracing the *de facto* length of the (unfolded or folded) cortical surface (Fig. 2E, green) over of a hypothetical minimal-length, i.e., smooth, tracing of the cortical surface (Fig. 2E, magenta) (*16*, *17*). Applying this tracing to the entire dorso-ventral dimension of the coronal sections analyzed, wild-type and *ARHGAP11B*-non-expressing neocortex exhibited a GI of nearly 1.0 (Fig. 2C), consistent with the essentially unfolded, near-lissencephalic nature of the marmoset neocortex (*18*, *19*). The GI of *ARHGAP11B*-expressing neocortex increased rostrally (Fig. 2C), and reached nearly 1.1 when the tracing was confined to the portion of the cortical surface where gyrus-like structures emerged (fig. S2, B and D). These structures did not arise by folding of a CP of equal thickness, but reflected local CP thickening (fig. S2, C to E), which in turn reflected a specific increase in upper-layer neurons as revealed by immunostaining for markers of specific neuron populations (fig. S2, D and F).

We then quantified CP thickness in wild-type, *ARHGAP11B*-non-expressing and *ARHGAP11B*-expressing marmoset neocortex, taking only regions where no gyrus-like structures emerged in the *ARHGAP11B*-expressing neocortex. This revealed increased CP thickness for *ARHGAP11B*-expressing neocortex as compared to wild-type and *ARHGAP11B*-non-expressing neocortex (Fig. 3, A and B, and figs. S3 and S4A).

To understand the basis of this increase in CP thickness, we quantified CP nuclei positive for Tbr1 and Ctip2, two markers of deep-layer neurons, and CP nuclei positive for Satb2 and Brn2, which are expressed by upper-layer neurons (*20*, *21*) (Fig. 3A and fig. S4B). We observed a nearly 40% and 50% increase in Satb2$^+$ neurons and Brn2$^+$ neurons, respectively, but not in Tbr1$^+$ and Ctip2$^+$ neurons, in the CP of *ARHGAP11B*-expressing marmoset neocortex as compared to wild-type and *ARHGAP11B*-non-expressing neocortex (Fig. 3C and fig. S4, C and D).

In line with the developmental stage of our analyses (fig. S1D), we noted that a substantial proportion of the Satb2$^+$ and Brn2$^+$ neurons observed in the cortical wall were found in the subplate (fig. S5, A and B), consistent with these neurons migrating to the CP (*22*, *23*). Accordingly, the numbers specifically of Satb2$^+$ and Brn2$^+$ neurons in the subplate were greater while subplate thickness was equal, for *ARHGAP11B*-expressing marmoset neocortex compared to wild-type and *ARHGAP11B*-non-expressing neocortex (fig. S5, C to F).

These data were consistent with an ongoing production of cortical neurons, mostly upper-layer neurons, at the developmental stage of our analyses (fig. S1D). We examined the germinal zones (VZ, iSVZ, oSVZ) and progenitors therein for wild-type, *ARHGAP11B*-non-expressing and *ARHGAP11B*-expressing marmoset neocortex (Fig. 4A). Analysis of the germinal zones showed increased oSVZ thickness for *ARHGAP11B*-expressing neocortex compared to wild-type and *ARHGAP11B*-non-expressing neocortex (Fig. 4B and fig. S7A). We observed an increase in mitotic basal progenitors that overall was ≈2-fold in the iSVZ and ≈3-fold in the oSVZ, but observed no difference in mitotic apical progenitors in the VZ (Fig. 4C and figs. S6 and S7, B and C).

At least half of the mitotic basal progenitors in the oSVZ of *ARHGAP11B*-expressing neocortex exhibited a basal process and hence were basal (or outer) radial glia (*24*–*27*), whereas this proportion was less (≤40%) for wild-type and *ARHGAP11B*-non-expressing neocortex (Fig. 4D and figs. S8, A to D), in line with previous data (*28*, *29*). *ARHGAP11B* expression increased mitotic basal radial glia ≈3-fold (Fig. 4E and fig. S8E). A significant increase in basal radial glia due to *ARHGAP11B* expression was also observed when these cells were quantified in interphase using the marker Hopx (*6*) (fig. S9). More than 99% of the mitotic basal radial glia in oSVZ were Sox2$^+$ (fig. S9F), and about half lacked expression of Tbr2 (Fig. 4, D and E, and fig. S8G). Hence, the cells amplified upon *ARHGAP11B* expression in fetal marmoset neocortex exhibited a marker signature consistent with the identity of basal radial glia (*5*, *6*, *9*).

In conclusion, we here examined physiologically relevant expression of human-specific *ARHGAP11B* (*7*, *8*) in the fetal neocortex of a non-human primate, the common marmoset, by using the human *ARHGAP11B* promoter, in contrast to previous studies that used a strong constitutive promoter (*9*, *10*).This expression increased fetal neocortex size, CP thickness, upper-layer neurons, oSVZ size (*14*), and basal progenitors, including basal radial glia, the progenitor type thought to drive development of the mammalian neocortex (*2*–*6*, *14*, *30*). Our results suggest that the human-specific *ARHGAP11B* gene may have caused neocortex expansion in the course of human evolution.

REFERENCES AND NOTES

1. P. Rakic, Evolution of the neocortex: A perspective from developmental biology. *Nat. Rev. Neurosci.* **10**, 724–735 (2009). doi:10.1038/nrn2719 Medline
2. J. H. Lui, D. V. Hansen, A. R. Kriegstein, Development and evolution of the human neocortex. *Cell* **146**, 18–36 (2011). doi:10.1016/j.cell.2011.06.030 Medline
3. M. Florio, W. B. Huttner, Neural progenitors, neurogenesis and the evolution of the neocortex. *Development* **141**, 2182–2194 (2014). doi:10.1242/dev.090571 Medline

4. C. Dehay, H. Kennedy, K. S. Kosik, The outer subventricular zone and primate-specific cortical complexification. *Neuron* **85**, 683–694 (2015). doi:10.1016/j.neuron.2014.12.060 Medline

5. Z. Molnár, G. J. Clowry, N. Šestan, A. Alzu'bi, T. Bakken, R. F. Hevner, P. S. Hüppi, I. Kostović, P. Rakic, E. S. Anton, D. Edwards, P. Garcez, A. Hoerder-Suabedissen, A. Kriegstein, New insights into the development of the human cerebral cortex. *J. Anat.* **235**, 432–451 (2019). doi:10.1111/joa.13055 Medline

6. D. L. Silver, P. Rakic, E. A. Grove, T. F. Haydar, T. K. Hensch, W. B. Huttner, Z. Molnár, J. L. Rubenstein, N. Sestan, M. P. Stryker, M. Sur, M. A. Tosches, C. A. Walsh, "Evolution and ontogenetic development of cortical structures," in *The Neocortex*, W. Singer, T. J. Sejnowski, P. Raki, Eds. (MIT Press, 2019), vol. 27 of Strüngmann Forum Reports, pp. 61–109.

7. P. H. Sudmant, J. O. Kitzman, F. Antonacci, C. Alkan, M. Malig, A. Tsalenko, N. Sampas, L. Bruhn, J. Shendure, E. E. Eichler; 1000 Genomes Project, Diversity of human copy number variation and multicopy genes. *Science* **330**, 641–646 (2010). doi:10.1126/science.1197005 Medline

8. M. Y. Dennis, L. Harshman, B. J. Nelson, O. Penn, S. Cantsilieris, J. Huddleston, F. Antonacci, K. Penewit, L. Denman, A. Raja, C. Baker, K. Mark, M. Malig, N. Janke, C. Espinoza, H. A. F. Stessman, X. Nuttle, K. Hoekzema, T. A. Lindsay-Graves, R. K. Wilson, E. E. Eichler, The evolution and population diversity of human-specific segmental duplications. *Nat. Ecol. Evol.* **1**, 0069 (2017). doi:10.1038/s41559-016-0069 Medline

9. M. Florio, M. Albert, E. Taverna, T. Namba, H. Brandl, E. Lewitus, C. Haffner, A. Sykes, F. K. Wong, J. Peters, E. Guhr, S. Klemroth, K. Prüfer, J. Kelso, R. Naumann, I. Nüsslein, A. Dahl, R. Lachmann, S. Pääbo, W. B. Huttner, Human-specific gene ARHGAP11B promotes basal progenitor amplification and neocortex expansion. *Science* **347**, 1465–1470 (2015). doi:10.1126/science.aaa1975 Medline

10. N. Kalebic, C. Gilardi, M. Albert, T. Namba, K. R. Long, M. Kostic, B. Langen, W. B. Huttner, Human-specific *ARHGAP11B* induces hallmarks of neocortical expansion in developing ferret neocortex. *eLife* **7**, e41241 (2018). doi:10.7554/eLife.41241 Medline

11. T. Namba, J. Dóczi, A. Pinson, L. Xing, N. Kalebic, M. Wilsch-Bräuninger, K. R. Long, S. Vaid, J. Lauer, A. Bogdanova, B. Borgonovo, A. Shevchenko, P. Keller, D. Drechsel, T. Kurzchalia, P. Wimberger, C. Chinopoulos, W. B. Huttner, Human-specific ARHGAP11B acts in mitochondria to expand neocortical progenitors by glutaminolysis. *Neuron* **105**, 867–881.e9 (2020). doi:10.1016/j.neuron.2019.11.027 Medline

12. M. Florio, T. Namba, S. Pääbo, M. Hiller, W. B. Huttner, A single splice site mutation in human-specific *ARHGAP11B* causes basal progenitor amplification. *Sci. Adv.* **2**, e1601941 (2016). doi:10.1126/sciadv.1601941 Medline

13. E. Sasaki, H. Suemizu, A. Shimada, K. Hanazawa, R. Oiwa, M. Kamioka, I. Tomioka, Y. Sotomaru, R. Hirakawa, T. Eto, S. Shiozawa, T. Maeda, M. Ito, R. Ito, C. Kito, C. Yagihashi, K. Kawai, H. Miyoshi, Y. Tanioka, N. Tamaoki, S. Habu, H. Okano, T. Nomura, Generation of transgenic non-human primates with germline transmission. *Nature* **459**, 523–527 (2009). doi:10.1038/nature08090 Medline

14. I. H. Smart, C. Dehay, P. Giroud, M. Berland, H. Kennedy, Unique morphological features of the proliferative zones and postmitotic compartments of the neural epithelium giving rise to striate and extrastriate cortex in the monkey. *Cereb. Cortex* **12**, 37–53 (2002). doi:10.1093/cercor/12.1.37 Medline

15. M. Florio, M. Heide, A. Pinson, H. Brandl, M. Albert, S. Winkler, P. Wimberger, W. B. Huttner, M. Hiller, Evolution and cell-type specificity of human-specific genes preferentially expressed in progenitors of fetal neocortex. *eLife* **7**, e32332 (2018). doi:10.7554/eLife.32332 Medline

16. K. Zilles, E. Armstrong, A. Schleicher, H. J. Kretschmann, The human pattern of gyrification in the cerebral cortex. *Anat. Embryol. (Berl.)* **179**, 173–179 (1988). doi:10.1007/BF00304699 Medline

17. K. R. Long, B. Newland, M. Florio, N. Kalebic, B. Langen, A. Kolterer, P. Wimberger, W. B. Huttner, Extracellular matrix components HAPLN1, lumican, and collagen I cause hyaluronic acid-dependent folding of the developing human neocortex. *Neuron* **99**, 702–719.e6 (2018). doi:10.1016/j.neuron.2018.07.013 Medline

18. K. Zilles, E. Armstrong, K. H. Moser, A. Schleicher, H. Stephan, Gyrification in the cerebral cortex of primates. *Brain Behav. Evol.* **34**, 143–150 (1989). doi:10.1159/000116500 Medline

19. K. Sawada, K. Hikishima, A. Y. Murayama, H. J. Okano, E. Sasaki, H. Okano, Fetal sulcation and gyrification in common marmosets (*Callithrix jacchus*) obtained by ex vivo magnetic resonance imaging. *Neuroscience* **257**, 158–174 (2014). doi:10.1016/j.neuroscience.2013.10.067 Medline

20. B. J. Molyneaux, P. Arlotta, J. R. Menezes, J. D. Macklis, Neuronal subtype specification in the cerebral cortex. *Nat. Rev. Neurosci.* **8**, 427–437 (2007). doi:10.1038/nrn2151 Medline

21. S. Lodato, P. Arlotta, Generating neuronal diversity in the mammalian cerebral cortex. *Annu. Rev. Cell Dev. Biol.* **31**, 699–720 (2015). doi:10.1146/annurev-cellbio-100814-125353 Medline

22. K. Y. Kwan, N. Sestan, E. S. Anton, Transcriptional co-regulation of neuronal migration and laminar identity in the neocortex. *Development* **139**, 1535–1546 (2012). doi:10.1242/dev.069963 Medline

23. O. Britanova, C. de Juan Romero, A. Cheung, K. Y. Kwan, M. Schwark, A. Gyorgy, T. Vogel, S. Akopov, M. Mitkovski, D. Agoston, N. Šestan, Z. Molnár, V. Tarabykin, Satb2 is a postmitotic determinant for upper-layer neuron specification in the neocortex. *Neuron* **57**, 378–392 (2008). doi:10.1016/j.neuron.2007.12.028 Medline

24. D. V. Hansen, J. H. Lui, P. R. Parker, A. R. Kriegstein, Neurogenic radial glia in the outer subventricular zone of human neocortex. *Nature* **464**, 554–561 (2010). doi:10.1038/nature08845 Medline

25. S. A. Fietz, I. Kelava, J. Vogt, M. Wilsch-Bräuninger, D. Stenzel, J. L. Fish, D. Corbeil, A. Riehn, W. Distler, R. Nitsch, W. B. Huttner, OSVZ progenitors of human and ferret neocortex are epithelial-like and expand by integrin signaling. *Nat. Neurosci.* **13**, 690–699 (2010). doi:10.1038/nn.2553 Medline

26. I. Reillo, C. de Juan Romero, M. A. García-Cabezas, V. Borrell, A role for intermediate radial glia in the tangential expansion of the mammalian cerebral cortex. *Cereb. Cortex* **21**, 1674–1694 (2011). doi:10.1093/cercor/bhq238 Medline

27. M. Betizeau, V. Cortay, D. Patti, S. Pfister, E. Gautier, A. Bellemin-Ménard, M. Afanassieff, C. Huissoud, R. J. Douglas, H. Kennedy, C. Dehay, Precursor diversity and complexity of lineage relationships in the outer subventricular zone of the primate. *Neuron* **80**, 442–457 (2013). doi:10.1016/j.neuron.2013.09.032 Medline

28. I. Kelava, I. Reillo, A. Y. Murayama, A. T. Kalinka, D. Stenzel, P. Tomancak, F. Matsuzaki, C. Lebrand, E. Sasaki, J. C. Schwamborn, H. Okano, W. B. Huttner, V. Borrell, Abundant occurrence of basal radial glia in the subventricular zone of embryonic neocortex of a lissencephalic primate, the common marmoset *Callithrix jacchus*. *Cereb. Cortex* **22**, 469–481 (2012). doi:10.1093/cercor/bhr301 Medline

29. F. García-Moreno, N. A. Vasistha, N. Trevia, J. A. Bourne, Z. Molnár, Compartmentalization of cerebral cortical germinal zones in a lissencephalic primate and gyrencephalic rodent. *Cereb. Cortex* **22**, 482–492 (2012). doi:10.1093/cercor/bhr312 Medline

30. V. Borrell, M. Götz, Role of radial glial cells in cerebral cortex folding. *Curr. Opin. Neurobiol.* **27**, 39–46 (2014). doi:10.1016/j.conb.2014.02.007 Medline

31. Y. Bai, Y. Soda, K. Izawa, T. Tanabe, X. Kang, A. Tojo, H. Hoshino, H. Miyoshi, S. Asano, K. Tani, Effective transduction and stable transgene expression in human blood cells by a third-generation lentiviral vector. *Gene Ther.* **10**, 1446–1457 (2003). doi:10.1038/sj.gt.3302026 Medline

32. T. Takahashi, K. Hanazawa, T. Inoue, K. Sato, A. Sedohara, J. Okahara, H. Suemizu, C. Yagihashi, M. Yamamoto, T. Eto, Y. Konno, H. Okano, M. Suematsu, E. Sasaki, Birth of healthy offspring following ICSI in in vitro-matured common marmoset (*Callithrix jacchus*) oocytes. *PLOS ONE* **9**, e95560 (2014). doi:10.1371/journal.pone.0095560 Medline

33. K. Sato, R. Oiwa, W. Kumita, R. Henry, T. Sakuma, R. Ito, R. Nozu, T. Inoue, I. Katano, K. Sato, N. Okahara, J. Okahara, Y. Shimizu, M. Yamamoto, K. Hanazawa, T. Kawakami, Y. Kametani, R. Suzuki, T. Takahashi, E. J. Weinstein, T. Yamamoto, Y. Sakakibara, S. Habu, J. Hata, H. Okano, E. Sasaki, Generation of a nonhuman primate model of severe combined immunodeficiency using highly efficient genome editing. *Cell Stem Cell* **19**, 127–138 (2016). doi:10.1016/j.stem.2016.06.003 Medline

ACKNOWLEDGMENTS

SUPPLEMENTARY MATERIALS
science.sciencemag.org/cgi/content/full/science.abb2401/DC1
Materials and Methods
Figs. S1 to S9
Tables S1 to S4
Data S1
References (*31–33*)
MDAR Reproducibility Checklist

10 February 2020; accepted 1 June 2020
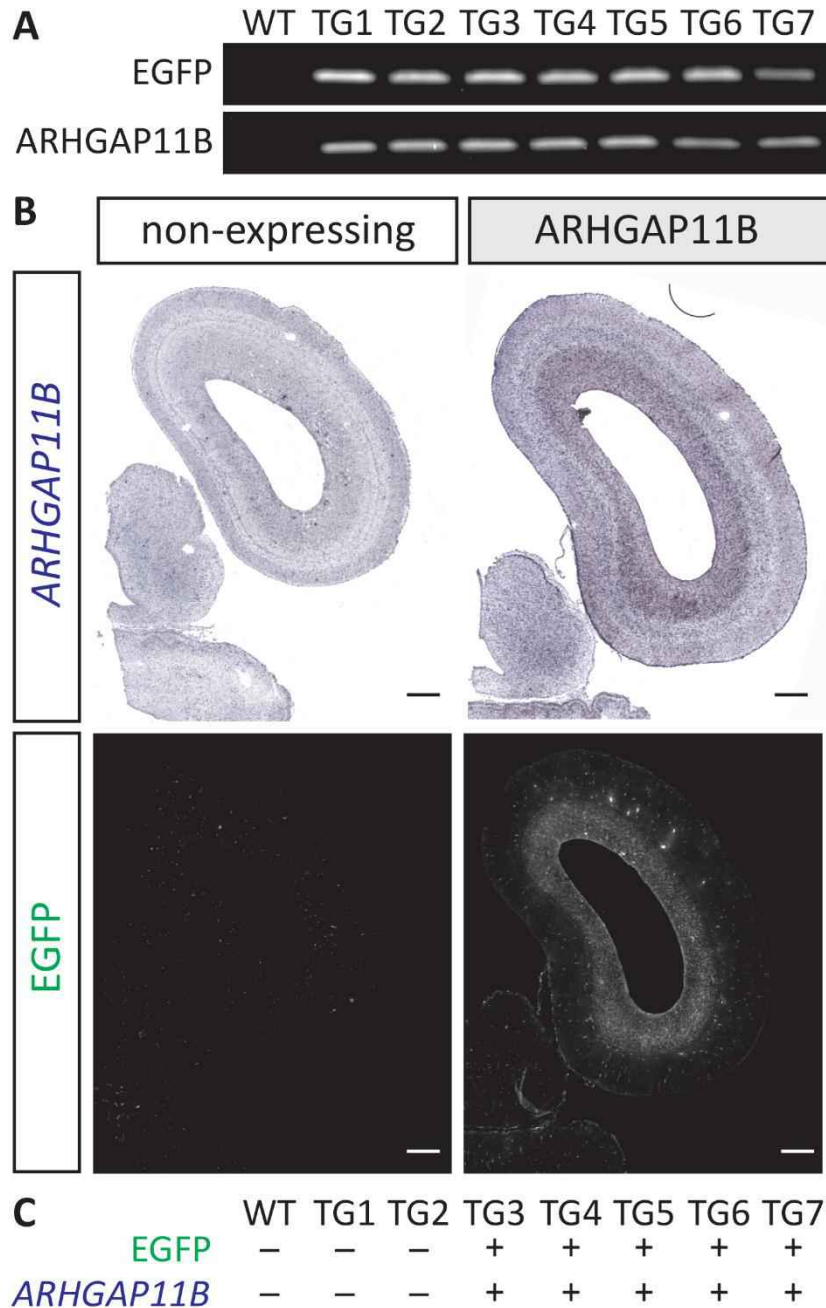Published online 18 June 2020
10.1126/science.abb2401

Fig. 1. *ARHGAP11B* and EGFP expression in *ARHGAP11B*-transgenic marmoset 101-day fetuses. Genomic PCR for *EGFP* and *ARHGAP11B* using somatic cells (**A**) and absence (−) or presence (+) of EGFP protein and *ARHGAP11B* mRNA expression (see **B**) in neocortex (**C**) of 1 wild-type (WT) and 7 *ARHGAP11B*-transgenic marmoset fetuses. (**B**) *ARHGAP11B* mRNA *in-situ*-hybridization (left) and EGFP immunohistochemistry (right) of *ARHGAP11B*-non-expressing (TG2) and *ARHGAP11B*-expressing (TG6) neocortex of marmoset fetuses. Scale bars, 500 μm.
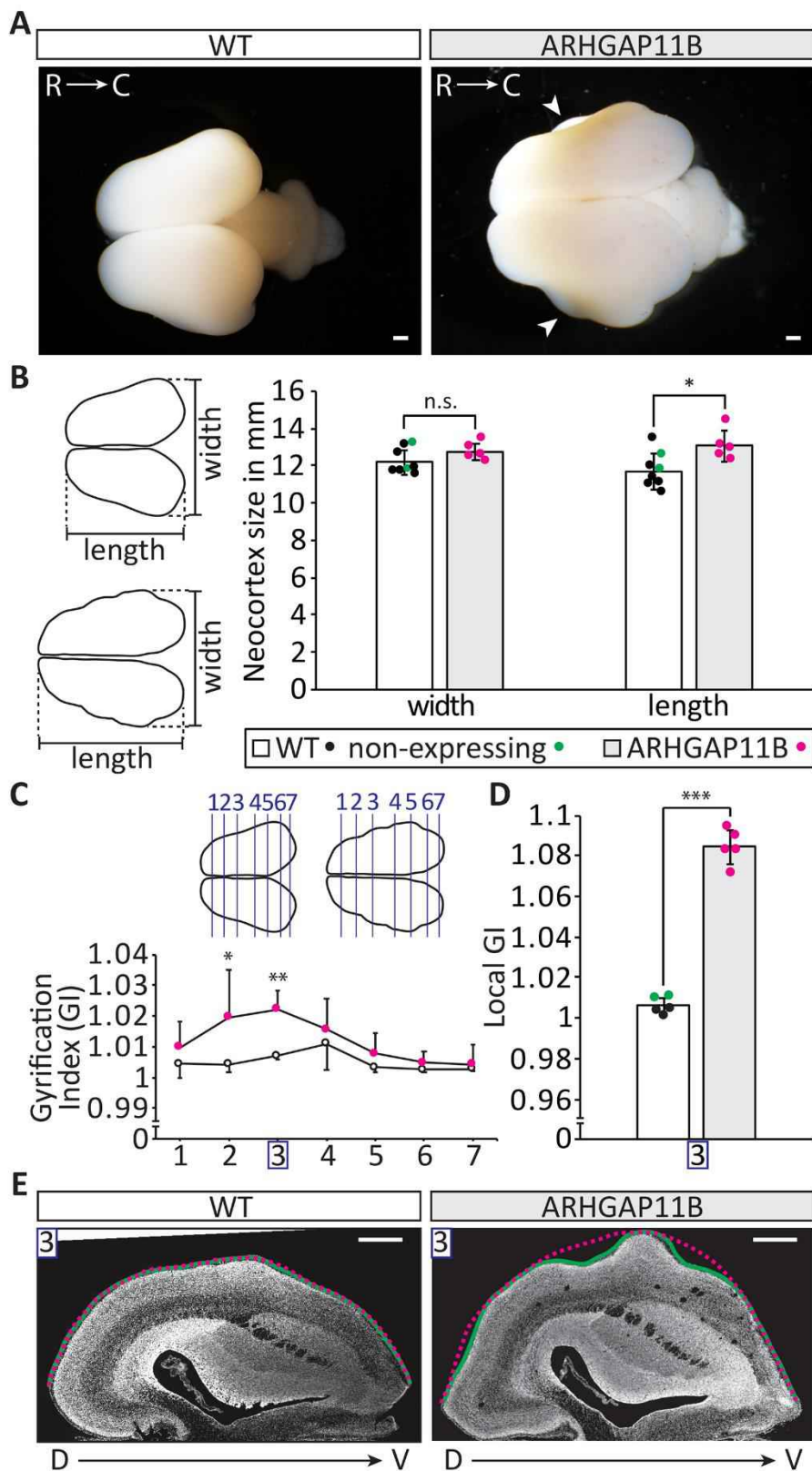
Fig. 2. Size and gyrification index of wild-type and *ARHGAP11B*-non-expressing vs. *ARHGAP11B*-expressing 101-day fetal marmoset neocortex. (**A**) Wild-type brain (WT) and brain expressing *ARHGAP11B* in neocortex (TG3). Arrowheads, cortical folds; R, rostral; C, caudal. Scale bars, 1 mm. (**B**) Width and length (see cartoons) of 6 wild-type (black dots, white columns) plus 2 *ARHGAP11B*-non-expressing (green dots, white columns) vs. 5 *ARHGAP11B*-expressing (magenta dots, grey columns) neocortices. Mean ± SD; n.s., not significant; *, $p < 0.05$ (two-tailed *t*-test). (**C**) Gyrification index (GI, see (**E**) and fig. S2A) of 3 wild-type plus 2 *ARHGAP11B*-non-expressing (white circles) vs. 5 *ARHGAP11B*-expressing (magenta circles) neocortices at 7 positions along the rostro-caudal axis (see cartoons). Data ± SD; *, $p < 0.05$; **, $p < 0.01$ (one-tailed *t*-test). (**D**) Local GI (see fig. S2B) of 3 wild-type (black dots, white column) plus 2 *ARHGAP11B*-non-expressing (green dots, white column) vs. 5 *ARHGAP11B*-expressing (magenta dots, grey column) neocortices. Mean ± SD; ***, $p < 0.001$ (two-tailed *t*-test). (**E**) DAPI-stained coronal section of wild-type (WT) and *ARHGAP11B*-expressing (TG4) neocortex at position 3 (see **C**). D, dorsal; V, ventral. Green line, *de facto* length of cortical surface; magenta line, hypothetical minimal length of cortical surface. Scale bars, 500 μm.
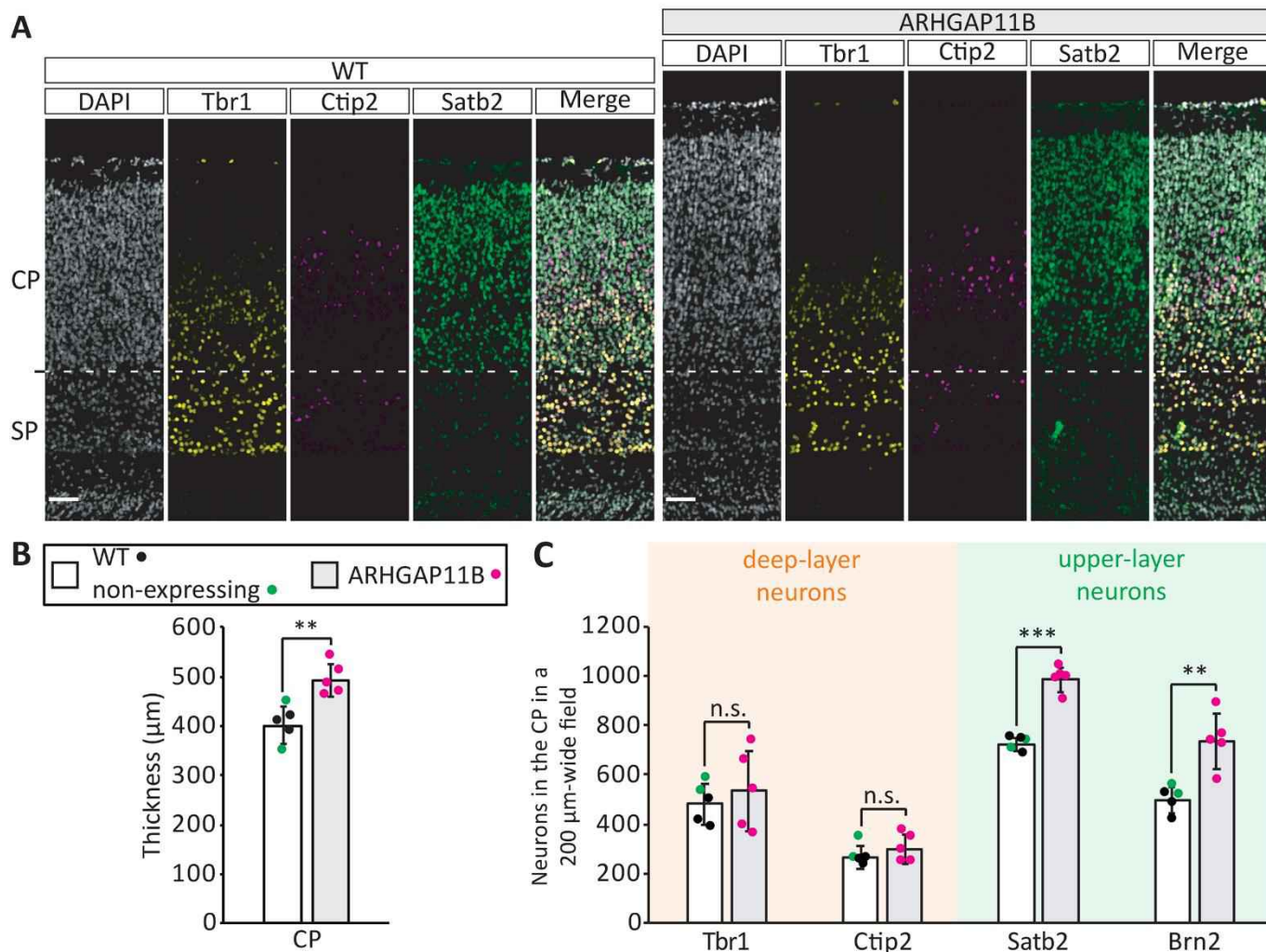
Fig. 3. *ARHGAP11B*-expressing 101-day fetal marmoset neocortex shows increased CP thickness and elevated numbers specifically of upper-layer neurons. (A) Triple immunofluorescence for Tbr1 (yellow), Ctip2 (magenta) and Satb2 (green), combined with DAPI staining (white), of wild-type (WT, left) and an *ARHGAP11B*-expressing (TG3, right) neocortex (occipital lobe). Scale bars, 50 µm. (B, C) CP thickness (B) and Tbr1+, Ctip2+ Satb2+ and Brn2+ neuron number in CP in 200 µm-wide field (C), of 3 wild-type (black dots, white columns) plus 2 *ARHGAP11B*-non-expressing (green dots, white columns) vs. 5 *ARHGAP11B*-expressing (magenta dots, grey columns) neocortices. For *ARHGAP11B*-expressing neocortex, quantification excluded gyrus. Mean ± SD; n.s., not significant; **, p<0.01; ***, p<0.001 (two-tailed *t*-test).
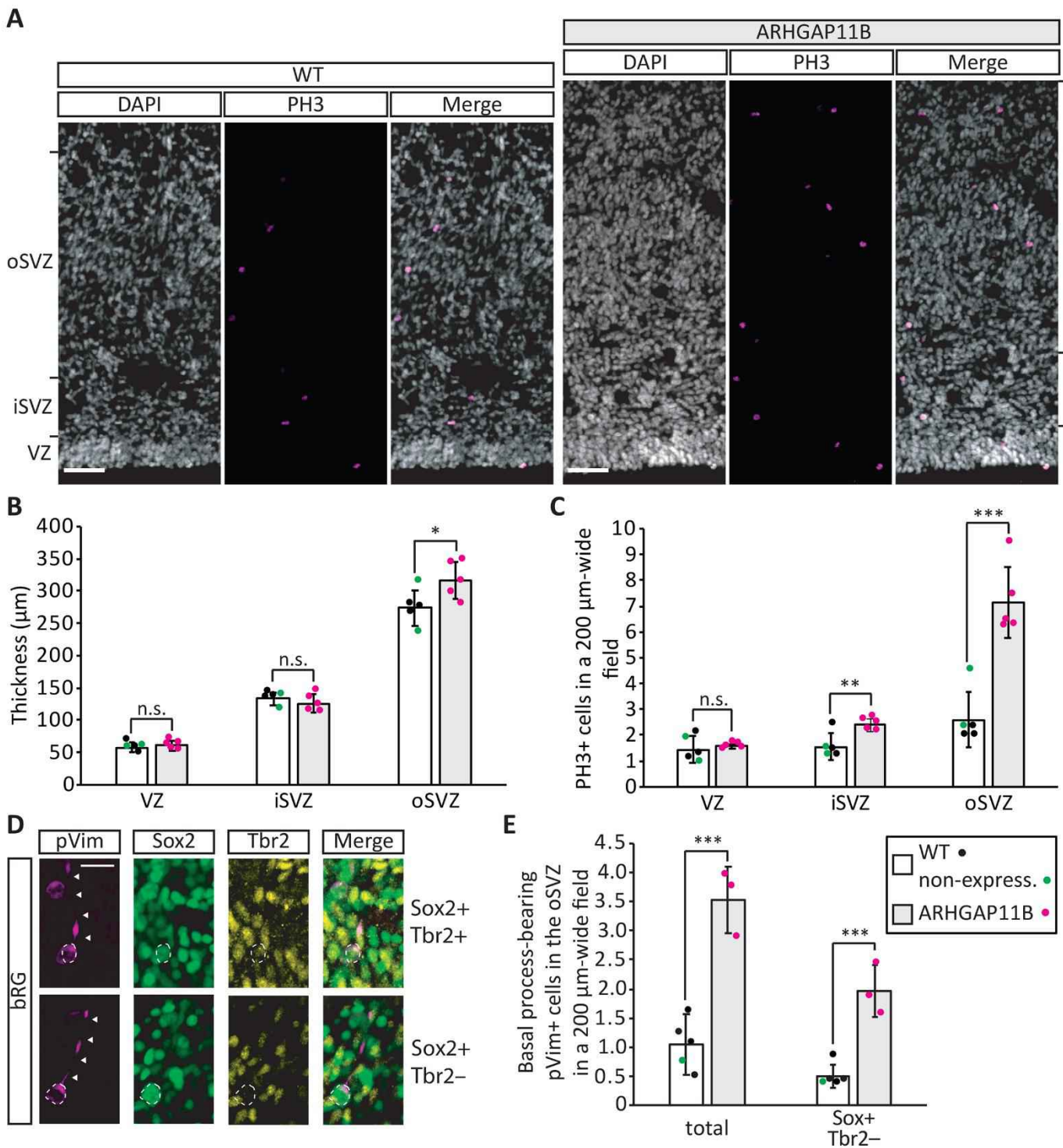
Fig. 4. *ARHGAP11B*-expressing 101-day fetal marmoset neocortex shows increased oSVZ thickness and elevated numbers of basal progenitors, notably basal radial glia. (**A**) Immunofluorescence for phosphohistone H3 (PH3, magenta), combined with DAPI staining (white), of wild-type (WT, left) and *ARHGAP11B*-expressing (TG6, right) neocortex (occipital lobe). Scale bars, 50 μm. (**B** and **C**) Germinal zone thickness (**B**) and PH3⁺ cell numbers in germinal zones in 200 μm-wide field (**C**), of 3 wild-type (black dots, white columns) plus 2 *ARHGAP11B*-non-expressing (green dots, white columns) vs. 5 *ARHGAP11B*-expressing (magenta dots, grey columns) neocortices. Mean ± SD; n.s., not significant; *, p<0.05; **, p<0.01; ***, p<0.001 (two-tailed *t*-test). (**D**) Triple immunofluorescence for phospho-vimentin (pVim, magenta), Sox2 (green) and Tbr2 (yellow) showing mitotic bRG in oSVZ of *ARHGAP11B*-expressing neocortex. Arrowheads, basal process. Top bRG shown is Sox2⁺ Tbr2⁺, bottom bRG is Sox2⁺ Tbr2⁻. Scale bars, 20 μm. (**E**) Numbers of total (left) and Sox2⁺ Tbr2⁻ (right) basal process-bearing pVim⁺ cells in oSVZ in 200 μm-wide field, of 4 wild-type (black dots, white columns) plus 1 *ARHGAP11B*-non-expressing (green dot, white columns) vs. 3 *ARHGAP11B*-expressing (magenta dots, grey columns) neocortices. Mean ± SD; ***, p<0.001 (two-tailed *t*-test).

Science

Human-specific *ARHGAP11B* increases size and folding of primate neocortex in the fetal marmoset

Michael Heide, Christiane Haffner, Ayako Murayama, Yoko Kurotaki, Haruka Shinohara, Hideyuki Okano, Erika Sasaki and Wieland B. Huttner

Use of this article is subject to the Terms of Service